

Evaluation of Load Path for Injury Prediction in Soft Tissues.

D. Kumar, S. Mukherjee, A. Chawla

I. INTRODUCTION

In automotive design, load paths have been conventionally used to identify and design structure members involved in progressive transfer of load from point of application to the point of reaction. This is a non-trivial exercise for non-homogeneous continuum as is encountered in FE-HBMs. This study demonstrates a methodology for estimating load path under impact through a FE human body model. Load path would be a useful tool to find changes in injury mechanism by identifying changes in organ loading when varying crash configuration.

II. METHODS

Load paths, conventionally used in automotive design [1] as shown in Fig. 1 for a front end crash, are indicative of members involved in transfer of load from point of application to the point of reaction. In Fig. 2 the multi-load path structure is shown, as adopted by Mazda for better crash safety performance. The structure efficiently absorbs the load at the time of a crash by dispersing it in multiple directions [2]. In the context of FE-HBMs, the load path is needed to identify injury mechanism by studying the sequence of organ loading. Changes induced in the load path by safety measures can be examined as a design assessment tool. In continuum, they are extracted from extremely-stressed contours in the local sense. These isolate locations where spatial stress gradients are small in one direction and large in the transverse direction. At such regions, the iso-stress contours are typically dense as compared to other regions. A MATLAB code has been used to extract load path in finite element mesh.

Currently injury prediction for FE-HBMs are based on instantaneous and point failure criteria, i.e., stress [3], strain[4-5] and Viscous Compression (VC).

Load path contours are identified as ridge points on a scalar map on 2D domain. Ridge points on higher dimensions are extracted by analysing the Hessian matrix. A tri-cubic (for 3-D) and bi-cubic (for 2D) equation is fitted to a scalar field on a localised patch of FE mesh using set of 16 nearest connected nodes for 2D and 64 nearest connected nodes for 3D. The first and second derivatives are evaluated to form the Hessian matrix, analysis of whose eigenvalues and eigenvectors yields candidate ridge points. Formally, following reference [6], let $U \subset \mathbb{R}^n$ be an open set, and $f: U \rightarrow \mathbb{R}$ be smooth. Let $x_0 \in U$. Let $\nabla_{x_0} f$ be the gradient of f at x_0 , and $H_{x_0}(f)$ be $n \times n$ Hessian matrix of f at x_0 . Let $\lambda_1 \leq \lambda_2 \leq \dots \leq \lambda_n$ be the n ordered eigenvalues of $H_{x_0}(f)$ and let e_i be the unit vector in the Eigen space for λ_i . The point x_0 is a *point on the k -dimensional ridge* of f if i) $\lambda_{n-k} \leq 0$ and ii) $(\nabla_{x_0} f) \cdot e_i = 0$ for $i = 1, 2, \dots, n - k$. For a function of n variables, its ridges are a set of curves whose points are local maxima in $n - 1$ dimensions. Some ridges are continuous curves extending to the boundary, and some may terminate at specific points called ridge endings. Sometimes two ridges coalesce at a point, called a bifurcation point. Ridge contours have been plotted for visualising the loading path in a transient 2D finite element mesh simulation.

III. INITIAL FINDINGS

An initially planar rectangular geometry with dimension 300x200x5mm thickness was created with density of 1.0e-6 kg/mm³, E of 22 MPa and poisson's ratio of 0.3, which is used in the THUMSD_OS_AM50_V4.0 Human Body Model for the human diaphragm. All boundary nodes were fixed; a load of 2N was applied perpendicular to the plate, on node 142 and 1N on node 259, both on interior of the geometry, as shown in Fig. 3. This was

D. Kumar (devendra87kumar@gmail.com, +91-9711017738) is a PhD student in the Department of Mechanical Engineering at Indian Institute of Technology, Delhi, India. S. Mukherjee and A. Chawla are Professors in Mechanical Engineering at Indian Institute of Technology, Delhi, INDIA.

simulated in ANSYS.

A MATLAB code was used to parse the nodal coordinate information, element to node connectivity and nodal Von-Mises stress to decide the candidature of a node to be a ridge node. Ridge lines would start from a boundary node, nearest ridge node searched within specified distance (Parameter 1 - say 3mm) and value of stress (Parameter 2) for next node should lie between $0.65 \times \text{stress}$ to $1.35 \times \text{stress}$ of previous node. The process is continued till all ridge points are exhausted. Further these ridge nodes are connected by cubic splines as shown in Fig. 4. Another case loading was done at four nodes while boundary nodes were fixed as shown in Fig. 5 and corresponding load-path is shown in Fig. 6

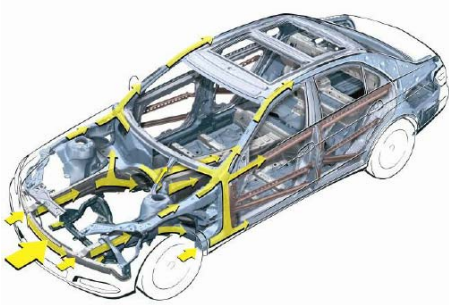


Fig. 1. Load paths (in yellow) during front-end crash.

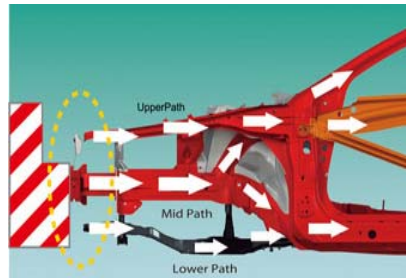


Fig. 2. Multi-load path structure.

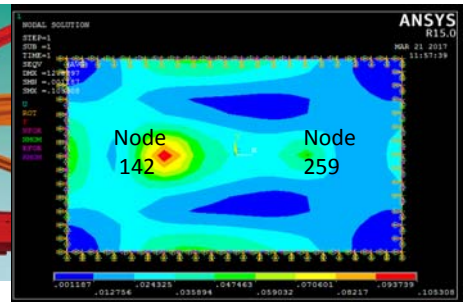


Fig. 3. Rectangle with two point load.

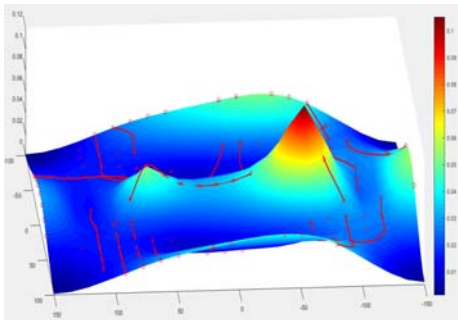


Fig. 4. Load paths (in red).

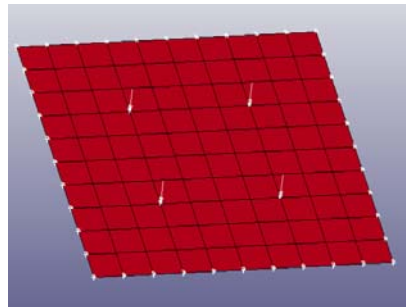


Fig. 5. Out of plane loading.

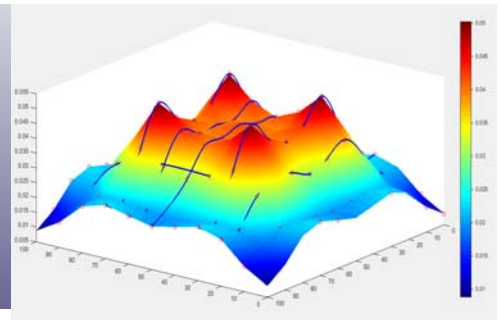


Fig. 6. Load paths (in blue).

IV. DISCUSSION

This paper shows a methodology for identifying tissues under extreme load, which are hence liable to fail structurally. This analysis reduces the zones to be tracked for injury assessment. The 3D extension of this work which will allow the loading path for finite element human body models organs to be identified is under progress. When applied to dynamically evolving frames typical of crash simulation, the time dependent load path can be identified. This could be used as a tool for design of safety structures along the same lines as load paths are used for crashworthiness design.

V. REFERENCES

- [1] C. M. Erdmann et al, SCT 2011. June, pp. 5–9.
- [2] "SKYACTIV TECHNOLOGY." [Online]. Available: <http://www.mazda.com/en/innovation/technology/skyactiv/skyactiv-body/>. [Accessed: 28-Mar-2017].
- [3] A. R. Kemper et al, AAAM, vol. 54, pp. 15–26, Jan. 2010.
- [4] A. J. Golman et al, Accid. Anal. Prev., vol. 64, pp. 1–8, Mar. 2014.
- [5] S. Umale et al, JMBBM, vol. 17, pp. 22–33, Jan. 2013.
- [6] D. Eberly et al, J. Math. Imaging Vis., vol. 4, no. 4, pp. 353–373, 1994.